European Journal of Phycology

ISSN: (Print) (Online) Journal homepage: www.tandfonline.com/journals/tejp20

Exploring the factors shaping microscopic morphological traits: insights from the chrysophycean genus *Synura* (Stramenopiles)

Iva Jadrná & Pavel Škaloud

To cite this article: Iva Jadrná & Pavel Škaloud (2025) Exploring the factors shaping microscopic morphological traits: insights from the chrysophycean genus *Synura* (Stramenopiles), European Journal of Phycology, 60:1, 67-83, DOI: 10.1080/09670262.2024.2442041

To link to this article: https://doi.org/10.1080/09670262.2024.2442041

EUROPEAN JOURNAL OF PHYCOLOGY
2025, VOL. 60, NO. 1, 67–83
https://doi.org/10.1080/09670262.2024.2442041

Exploring the factors shaping microscopic morphological traits: insights from the chrysophycean genus *Synura* (Stramenopiles)

Iva Jadrná and Pavel Škaloud

Faculty of Science, Department of Botany, Charles University, Benátská 2, Prague, 128 00 Praha 2, Czech Republic

ABSTRACT

Synura represents a common freshwater protist genus known for producing morphologically diverse silica scales with species-specific secondary structures. In this study, we analysed 19 scale-bearing morphological traits across over 700 genetically verified records, spanning a broad environmental gradient in Europe. Focusing on *Synura* from section *Petersenianae*, we identified 29 species-level lineages, 13 of which had not been previously described. Interestingly, while species diversity increased northwards, morphological trait diversity exhibited the opposite trend, being higher in southern Europe. This suggests that abiotic factors play a significant role in shaping these traits, which are differently responsive to gradients than taxonomic diversity. We observed non-random distribution of scale morphological traits, influenced by abiotic factors such as temperature, precipitation and pH. Scale elongation appears to be an adaptation for living in oligotrophic waters with reduced sunlight availability, while the increasing distance between struts likely reflects an adaptation to low silica concentrations. Notably, specific morphological traits may provide more informative insights into environmental drivers than taxonomic units. The study sheds light on the intricate relationship between environmental conditions and the morphology of silica scales, emphasizing the importance of considering both taxonomic and morphological diversity in ecological research.

HIGHLIGHTS

- Nanostructures of *Synura* silica scales represent unique morphological traits in protists.
- The distribution of microscopic traits on silica scales correlates with abiotic factors such as temperature, precipitation and pH.
- Specific morphological traits may provide more informative insights into environmental drivers than taxonomically based units.

ARTICLE HISTORY Received 17 August 2024; Revised 20 November 2024; Accepted 1 December 2024

KEYWORDS Biogeography; Chrysophyceae; morphological traits; protist; silica scales; speciation; *Synura*

Introduction

The factors that shape the regional species pool have been the subject of countless studies, revealing that abiotic, biotic and historical factors matter to varying degrees depending on the organism under study (Fernández *et al.*, 2017; Zhang *et al.*, 2018; Plante *et al.*, 2021). Moreover, the presence of stochasticity in these processes plays a part. Although multiple factors influence species diversity and abundance simultaneously, an organism's traits are what ultimately decide whether or not it will exist in a particular habitat (Salzburger, 2009; Pigot *et al.*, 2020; Westerband *et al.*, 2021). Therefore, revealing the characteristics of organisms that are important in terms of increasing their fitness or at least allowing them to survive should be at the centre of our attention.

Every characteristic of an organism is unique and has varying degrees of importance for their development. We assume that only species with certain morphological and physiological characteristics related to fitness or performance, often described as functional traits (Violle *et al.*, 2007), may tolerate environmental conditions and can persist in a given environment, while others are excluded. In other words, the restricted range of organisms with certain traits is considered as evidence of filtering processes, primarily driven by abiotic factors (Ackerly & Cornwell, 2007). However, the functional traits exhibit variation both along environmental gradients and among organisms inhabiting similar conditions, making the system much more complex (Lamanna *et al.*, 2014; Hurtado *et al.*, 2020). Nevertheless, a major advantage of the trait-based approach is its independence from taxonomic units, which makes it both robust and versatile, and it has thus been used to address a wide range of evolutionary and ecological questions not only in plants and animals (Violle *et al.*, 2007), but also in microorganisms (Green *et al.*, 2008).

Identifying the functional traits that define the ecological niches of organisms can be tricky. Many traits are correlated and closely linked, leading to limitations in their combinations and the need to find trade-offs between these traits, making the

CONTACT Pavel Škaloud skaloud@natur.cuni.cz

assessment of a given trait challenging (Follows *et al.*, 2007; Merico *et al.*, 2009). In contrast to plants and animals, microorganisms face an additional challenge due to their tiny size, which restricts the number of morphological traits available for study. Key traits generally recognised as important to determine the presence of a microorganism in a given niche are those closely related to its ability to grow and reproduce, such as cell size, genome size, gene content and mutation rate (Green *et al.*, 2008).

One of the important groups of microorganisms is phytoplankton, which consist of tiny, single-celled, filamentous or colonial organisms that play many crucial roles in aquatic ecosystems, including oxygen production, serving as a base of the food web, and the regulation of nutrient cycles. Phytoplankton functional traits explaining responses to environmental gradients were proposed to include aspects related to life history (the ability to reproduce and form resting stages), behavioural characteristics (motility), physiological processes (metabolism, nitrogen fixation, toxin production) and morphological variations (cell size and shape, coloniality) (Litchman & Klausmeier, 2008). Other important functional traits include those that enable algae to cope with stress, resist viral infection or grazing (Pančić & Kiørboe, 2018).

However, studies on the functional traits of microorganisms almost completely neglect submicroscopic structures such as siliceous or calcareous scales and skeletons, yet they are known for their extraordinary variety and complexity. It was hypothesised that these inorganic cases may increase the resistance against water pressure (Knotek & Škaloud, 2023), offer protection against predators and parasites (Pančić *et al.*, 2019), and scatter the light to stimulate photosynthesis or reflect UV light away from the cell (Goessling *et al.*, 2021). However, the adaptive function of the size, shape and patterns of the scales and skeletons is largely unknown. Here, we hypothesised that scale morphology may serve as an easily identifiable proxy associated with the fitness or performance of their carrier species. Furthermore, identifying adaptive traits can assist us in estimating a species' fundamental niche and predicting how community structure will alter in response to stress such as climate change.

The aim of this study is to investigate the putative adaptive role of siliceous scale morphological features as functional traits shaping the distribution and environmental preferences of phytoplankton species, using the freshwater algal genus *Synura* (Chrysophyceae, Stramenopiles) as a model. *Synura* forms motile colonies, with individual cells connected by tails in the colony centre and covered with a layer of overlapping siliceous scales. The scales are typically up to 10 in μm length, consisting of a perforated basal plate with pores, an upturned rim that encircles half to two-thirds of the scale, and various species-specific secondary structures (Škaloud *et al.*, 2013). The taxonomy of the genus *Synura* is currently well resolved, supported by morphological, molecular and ecological characters, with approximately 62 accepted species divided into the sections *Synura, Curtispinae* and *Peterseniane* (Jo *et al.*, 2016). Here, we specifically focus on the section *Petersenianae*, employing a long-term database of species distributions across Europe, comprising over 700 genetically verified records. The scales of these species are variable in size and shape, ranging from circular to long lanceolate, with a characteristic raised elongated ridge (keel) positioned in the middle of the scale, and fixed to the basal plate by radially arranged struts (Fig. 1). Moreover, each species has several morphological scale types, categorized by their position on the cell of the algae, and so they can be sorted as apical, body (usually used for species description) or caudal scales.

Materials and methods

Collection, isolation and cultivation of Synura *strains*

The database of the *Petersenianae* species occurrences was created on the basis of extensive European

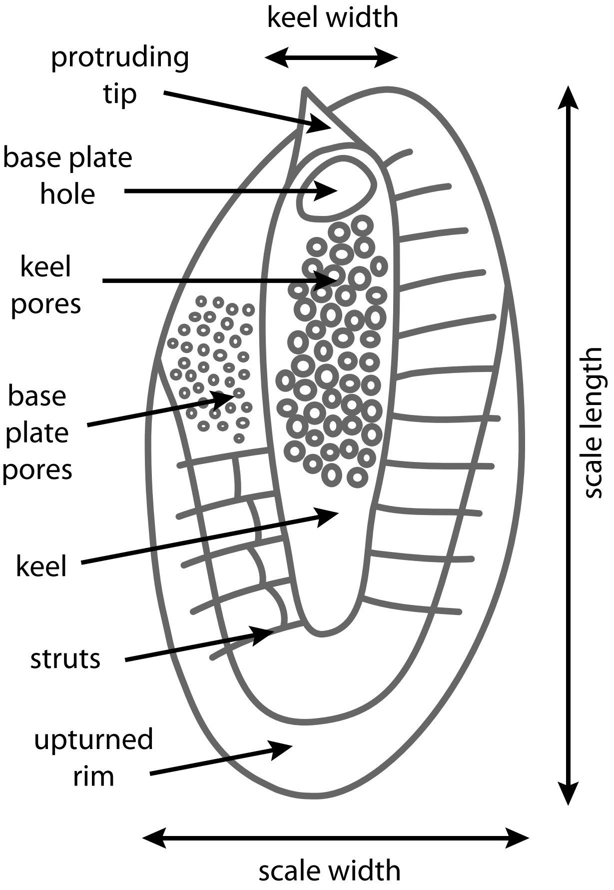

Fig. 1. Morphological traits of silica scales measured in *Synura* species.

sampling that took place between 2007 and 2024 (Supplementary table S1). Plankton samples were collected from various habitats in a total of 25 European countries (Austria, Belgium, Bulgaria, Croatia, Czech Republic, Denmark, Estonia, Finland, France, Germany, Great Britain, Greece, Hungary, Ireland, Lithuania, the Netherlands, Norway, Poland, Portugal, Romania, Slovakia, Slovenia, Spain, Sweden, Ukraine) using a plankton net with 10 µm mesh. At each sampling site, abiotic factors such as pH, conductivity and water temperature were measured using a combined pH/conductivity instrument (WTW 340i; WTW GmbH). Samples were examined with an Olympus CH light microscope, and the individual *Synura* colonies were isolated by micropipetting to establish monocolonial cultures. Each colony was placed into a separate well of a 96-well polypropylene plate filled with approximately 300 µm of liquid WC medium (Boenigk *et al.*, 2006), and the plates were cultivated at 14°C under constant illumination of 40 µmol photons m^{-2}. s^{-1} (TLD 18 W/33 fluorescent lamps; Philips). After 3–4 weeks the wells were checked using an inverted microscope Leica DMi1 and 100 µl of the culture were harvested. Over the period specified above, a total of 3846 *Synura* cultures were successfully isolated from 754 sampled sites. Of these, a total of 2554 cultures were genetically identified (see below) to belong to the section *Peterseniane*. As multiple isolates of the same species were often obtained from a single locality, the total number of unique European species occurrences was 769. Our collection was further supplemented by four strains ordered from algal culture collections SAG (strain 120.79), NIES (strain 1007) and ACOI (strains 1259 and 1707), and six strains isolated outside Europe (CNU01, I7, I15, Nojeok020610A, Sotan012410A, T83) for which either additional loci or morphological data were already obtained.

Sequencing, phylogenetic analyses and species delimitation

For DNA isolation, the harvested cultures were centrifuged for 5 min at 5000 rpm, and 30 µl of InstaGene matrix (Bio-Rad Laboratories) was added to the pellet and processed following the guidelines provided by the manufacturer. All strains were genetically characterised by sequencing ITS rDNA, which has been shown to represent an ideal DNA barcode to distinguish among *Synura* species (Škaloud *et al.*, 2020). After the identification of strains belonging to *Peterseniane*, we additionally sequenced *cox*I and *rbc*L genes for the selection of strains having a unique ITS rDNA barcode to obtain robust, well-resolved phylogeny. PCR amplifications were performed in 10 µl reaction volumes (6.7 µl sterile water, 2 µl MyTaq^{TM} Buffer (Bioline), 0.1 µl of each forward and reverse primers, 0.1 µl MyTaq^{TM} DNA polymerase (5 U $µl^{-1}$, Bioline) and 1 µl DNA template) using Eppendorff Mastercycler EP Gradient S PCR Thermal Cycler. Used primers are listed in Supplementary table S2. The amplified PCR products were quantified using a 0.8% agarose gel stained with GelGreen (Biotium) and purified using ExoSAP-IT™ PCR Product Cleanup Reagen (Applied Biosystems) and sequenced with an ABI3730XL DNA Analyser at Macrogen Europe in Amsterdam, the Netherlands.

The sequences were aligned using MAFFT v6, applying the Q-INS-i strategy (Katoh *et al.*, 2002). First, we inferred the maximum-likelihood phylogeny of all sequenced strains in IQ-TREE v. 1.6.1 (Nguyen *et al.*, 2015) using GTR+I + G substitution model. We then selected all unique ITS rDNA genotypes and prepared a concatenated alignment supplemented with *cox*I and *rbc*L manually aligned gene sequences. Second, we inferred the ultrametric tree using the BEAST v.1.10.4 (Suchard *et al.*, 2018) under the assumption of an uncorrelated lognormal relaxed molecular clock and speciation birth-death process tree prior. The analyses were performed on partitioned datasets using the different substitution models selected using the Bayesian information criterion (BIC) implemented in jModelTest 2.1.10 (Darriba *et al.*, 2012). The following models with the lowest BIC scores were selected: (1) GTR + G for ITS1 and ITS2 rDNA, (2) JC for 5.8S rDNA and the second *rbc*L and *cox*I codon partitions, (3) GTR + I for the first and third *rbc*L codon partitions and (4) GTR + I + G for the first and third *cox*I codon partitions. Three MCMC analyses were run for 50 million generations, sampling every 5000 generations. The outputs were diagnosed for convergence using TRACER v.1.7.1 (Rambaut *et al.*, 2018). Consensus trees were generated using TreeAnnotator v.1.10.4. The phylogenetic trees were inferred for both all taxa included and without the genetically distant *S. asmundiae*, *S. bjoerkii* and *S. macracantha*.

Four different approaches were used for delimiting OTUs based on sequence data: GMYC analysis, a Bayesian implementation of PTP approach (bPTP) (Zhang *et al.*, 2013), Automatic Barcode Gap Discovery method (ABGD) (Puillandre *et al.*, 2012) and a Bayesian species delimitation STACEY (Jones, 2016). GMYC analysis was performed on the BEAST-generated ultrametric tree under the single-threshold model, using the SPLITS package (Ezard *et al.*, 2009) in R v.4.4.0 (R Core Team, 2020). The bPTP analysis was conducted on the bPTP web server (http://species.h-its.org/ptp/), using the same ultrametric tree with 500 000 MCMC generations and burn-in set to 0.2. The ABGD analysis was performed on the ABGD website (https://bioinfo.mnhn.fr/abi/public/abgd/abgdweb.html), using P_{min} = 0.001, P_{max} = 0.1), Steps = 10 and Nb bins = 20. We chose Jukes–Cantor 1969 (JC69) model of DNA evolution and performed three analyses with different values of relative gap width (X set to 0.1, 0.5 and 1.0). All three analyses outputted the identical species scenario. Finally, the STACEY analysis was performed in the BEAST2 v.2.5.0 (Bouckaert *et al.*, 2019) template Stacey, using the same partitioned dataset, clock and tree models described above for the BEAST analysis, without a priori defined minimal clusters. The priors were modified by setting the bdcGrowthRate to lognormal (5,2), clockRate of all partitions to lognormal (0,1), popPriorScale to lognormal (−7,2), and relative Death Rate Species to Beta (1,1000). Three MCMC analyses were run for 100 million generations, sampling every 5000 generations. The outputs were diagnosed for convergence using TRACER v.1.7.1 (Rambaut *et al.*, 2018) and the species trees were combined using TreeAnnotator v.2.5.0, with a 20% burn-in. The Species Delimitation Analyser (Jones *et al.*, 2015) was used to process output files and to examine the clusters of species assignments under three different values of collapse height parameters (0.001, 0.05, 0.01). All three runs outputted the identical species scenario.

Morphological analyses

With the exception of two lineages comprising just three occurrences, all species and species-level lineages delimited by the approach described above were morphologically characterised by detailed measurements of their silica scales. Each lineage was characterised by measuring 1–2 strains in which a minimum of 10 but usually 20 scales were measured. Morphological traits of several *Peterseniianae* species were derived from Jadrná *et al.* (2021), and then it was supplemented by additional measurements of cultivated strains grown in liquid WC medium in 50 ml Erlenmeyer flasks. The living cultures were dropped onto Formvar-coated copper grids, and after drying, they were washed in three drops of distilled water. After further drying, they were examined with a JEOL 1011 transmission electron microscope equipped by CCD camera Veleta (Olympus Soft Imaging Solution GmbH). The body scales, which are standardly used for species delimitation, were measured using ImageJ 1.46 r (Rasband, 1997). The following morphological traits were measured: scale length, width, perimeter, area and roundness; upturned rim width, length and area; keel length, width and area; base hole area; length of a protruding tip (part of the keel measured from its attachment to the base plate pore to its tip); number and distance between struts; keel pore area; base plate pore area. As a result, we measured a total of 19 morphological traits in 24 taxa (Supplementary table S3). The five very rare taxa that we molecularly characterised unfortunately died before we were able to obtain at least 20 scales for morphological analyses. These lineages were therefore excluded from further analyses. For subsequent analyses, we reduced the number of traits by performing a correlation analysis using Pearson's correlation coefficients, selecting six non-correlated morphological traits that may be influenced by ecological variables by hierarchical clustering using the 'CorrPlot' package in R (Wei & Simko, 2021; Supplementary fig. S1). These include scale length, scale width, scale roundness, base hole area, keel pore area and strut distance.

Statistical analyses

Environmental data were obtained for each analysed site with the exception of 20 localities where pH and conductivity values were not acquired. The climatic data were obtained from the CHELSA v2.1 Climatologies database (Karger & Zimmermann, 2021) with long-term mean values for the period 1981–2010. Habitat factors were represented by measured values of pH and conductivity (ionic content), and by seven physical and chemical soil properties obtained from the SoilGrids 2.0 database (Poggio *et al.*, 2021). At every sampling site, climatic and habitat data were obtained by applying a 2-km buffer to limit the effects of spatial bias. To reduce the number of predictors, we carried out a correlation analysis using Pearson's correlation coefficients and identified significantly correlated variables by hierarchical clustering using the 'CorrPlot' package in R (Wei & Simko, 2021; Supplementary fig. S2). As a result, a total of 15 variables were selected: annual mean temperature (bio1), mean diurnal range (bio2; mean diurnal range of temperatures averaged over 1 year), temperature seasonality (bio4; standard deviation of the monthly mean temperatures), annual precipitation (bio12), precipitation seasonality (bio15), net primary productivity (npp), climate moisture index (cmi; average monthly climate moisture index over 1 year), mean monthly near-surface wind speed (sfc), amount of liquid water if snow is melted (swe), soil sand content (sand), soil silt content (silt), soil clay content (clay), soil organic carbon content (occ), pH and conductivity.

With the set of 15 selected variables, we then performed the model selection using the 'Mumin' package in R (Bartoń, 2020). First, we fitted a full model with the whole set of predictors for each phenotypic trait. Then, we performed an all-subsets model selection based on AIC$_c$ (Second-order Akaike Information Criterion), comparing models with all combinations of predictors using the dredge() function. Since there was little difference in the AIC and weights of the first best models, we summarised the outputs of these models using the strategy published by Mašková *et al.* (2022). First, we subsampled all models that differed from the best model by less than two Akaike units. Then, the relative importance of each environmental predictor was estimated by the sum of the AIC_c weights of the models in which the given predictor appeared, divided by the sum of the AIC_c weights of all models. Finally, the standardised regression coefficients and their confidence intervals were for each predictor determined by computing their Akaike-weighted means (exp(−0.5) * deltaAIC_c values) from all models that included that term. The regression coefficient plots were generated using the 'ggplot2' package in R (Wickham *et al.*, 2019). For phenotypic traits where the top model outputted high R^2 values, we also generated the linear regression plots with selected predictors using the lm() function in R.

The climatic niche hypervolumes were constructed in R, using the hypervolume (Blonder *et al.*, 2014) and alphahull (Pateiro-Lopez & Rodriguez-Casal, 2016) packages. First, we performed the PCA analysis of the set of 15 environmental variables (see above) measured at all sampling sites. The first two PCA axes (explaining 55% of the total variance) were then selected to calculate species' hypervolumes. The boundaries of the kernel density estimates were delineated by the probability threshold, using the 0.85 quantile value. To project the niche spaces of particular lineages, hypervolume contours were plotted based on 1000 random background points, using the alphahull contour type and alpha smoothing value 0.55.

The distribution maps were produced in R. The map of Europe was downloaded from GISCO API – Eurostat, using the packages 'giscoR' (Hernangómez & Arel-Bundock, 1995) and 'tidygeocoder' (Cambon *et al.*, 2021). Then, the hexagonal grid was created based on the map shapefile using the packages 'sf' (Pebesma & Bivand, 2023), with the cell size of 400 km. After checking the correspondence between hexagonal grid coordinates and species occurrence, we estimated species occurrences and diversity, overall morphological diversity, and the mean value of morphological traits in each hexagon, and plotted the coloured hexagonal grids using the package 'ggplot2' (Wickham *et al.*, 2019). Species diversity was calculated by both simply summing the number of species and by estimating the Shannon–Wiener diversity indices in each grid. Overall morphological diversity was calculated by averaging the variances of all 19 morphological traits measured, which were first standardised by z-score normalisation. Distribution maps of individual morphological traits were made by averaging the trait values of all species found in a given grid. Finally, we measured the cell dimensions in 11 selected species in which we maintain live cultures and calculated the relationship between scale length-to-width ratios and cell length-to-width ratios, which was analysed by fitting a linear model in R.

Results

Species and trait diversity

We analysed a total of 769 *Synura* occurrences across Europe, spanning a wide variety of environmental and habitat conditions (pH varying from 4 to 10, conductivity from 11–3000 µS cm^{-1}, mean annual air temperature from −0.6–17.4°C, annual precipitation from 463–-3425 kg m^{-2}, net primary productivity from 602–1773 g C m^{-2} yr^{-1}). ITS rDNA barcoding identified a total of 86 genotypes, which were grouped into 29 species or species-level lineages based on the species delimitation analyses (Fig. 2). Four different species delimitation analyses generally resulted in the same clustering of genotypes, although in some cases the analyses disagreed. The greatest disagreement was in the delimitation of *S. borealis*. We ultimately defined species lineages conservatively as the smallest number of clearly separable clusters. In several species (*S. americana*, *S. conopea*, *S. glabra* and *S. petersenii*), we detected the presence of intragenomic variations in the ITS rDNA repeats, as reflected by the presence of double peaks at given nucleotide positions. After filtering out this variability, all isolates of the given species were completely identical in their ITS rDNA sequence. Interestingly, some of these genotypes were so genetically distinct that some species delimitation analyses wrongly identified them as separate species lineages.

There are 13 species-level lineages that have not been formally described. These lineages mainly form a cluster affiliated with *S. borealis*, as well as two clusters sister to *S. soroconopea* and *S. macropora*, respectively (Fig. 2). All of these lineages are rare in their distribution, being found in only 5% of cases. The most abundant species were *S. petersenii* and *S. glabra*, found in more than one half (57%) of cases. Typically, in a given locality, up to three species co-occur, but in some cases, there have been as many as six species observed. Of the eight most abundant species, five (*S. petersenii*, *S. glabra*, *S. heteropora*, *S. americana* and *S. macropora*) share the climatic niches, with no obvious distributional differences (Fig. 3a). *S. hibernica* is restricted in its distribution to western Ireland, occupying a narrow climatic niche defined by high annual precipitation and climate moisture index (Fig. 3b–d). *S. conopea* has a broad climatic niche but shifted to prefer sites with low conductivity and pH (Fig. 3b, 3c, 3e). Finally, *S. borealis* shows a narrow climatic niche, occupying sites with low annual temperature, high temperature seasonality and high soil sand content (Fig. 3b, 3c), being restricted to northern Europe (Fig. 3f).

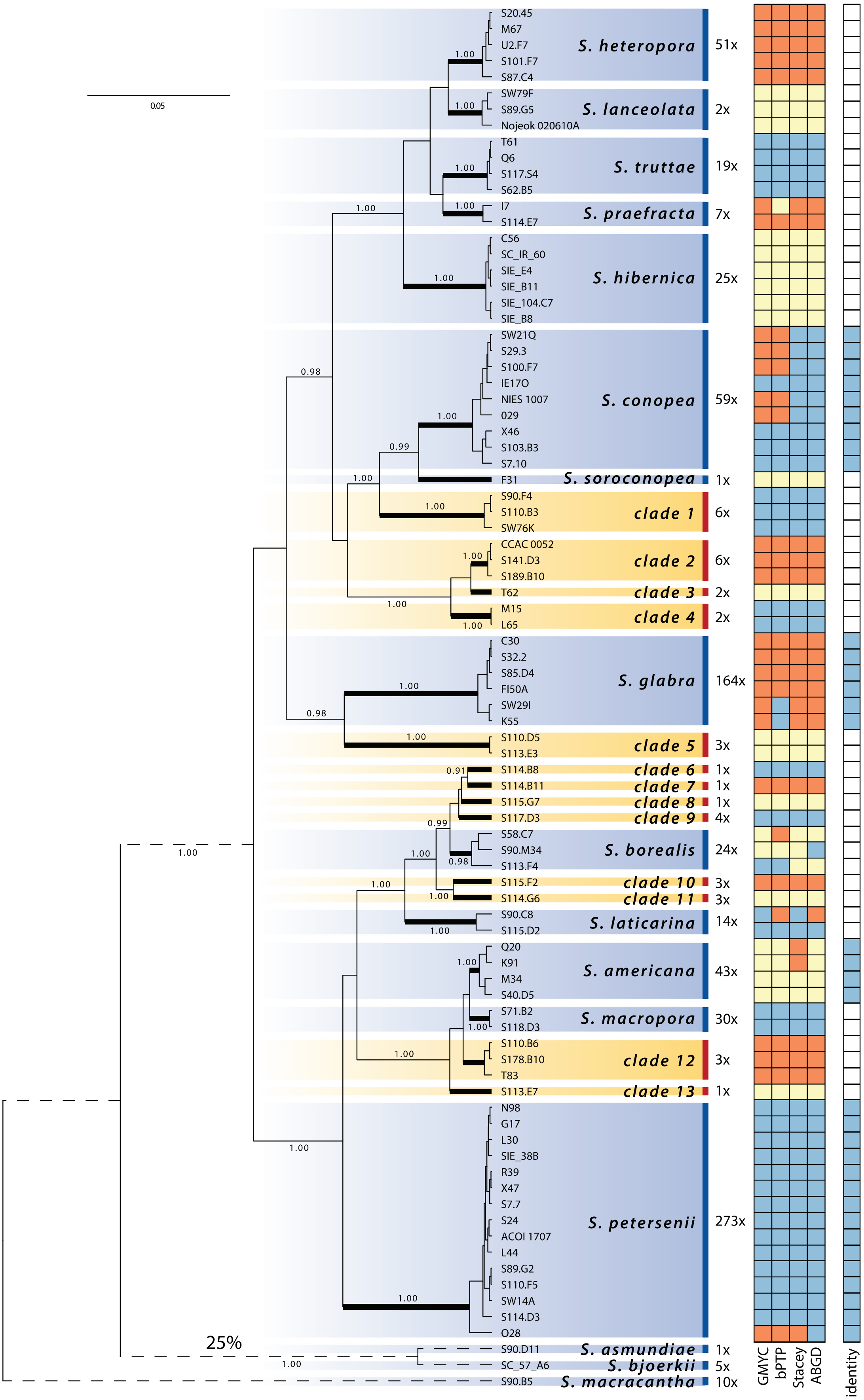

Fig. 2. Bayesian phylogenetic tree of all obtained genotypes within the genus *Synura*, section *Peterseniane* obtained by the concatenated BEAST analysis of *cox*I, *rbc*L and ITS rDNA loci. Values at the nodes indicate Bayesian posterior probabilities; only values higher than 0.95 are shown. Dashed branches were truncated to a quarter of their original length. Scale bar shows the estimated number of substitutions per site. The results of four species delineatation analyses (GMYC, bPTP, Stacey and ABGD) are shown along the tree, with the finally delimited species indicated by thick branches. The numbers represent the total number of individuals belonging to the species. In the rightmost column of the grid (identity), coloured cells indicate genetically identical genotypes after filtering out the ITS rDNA intragenomic variability.

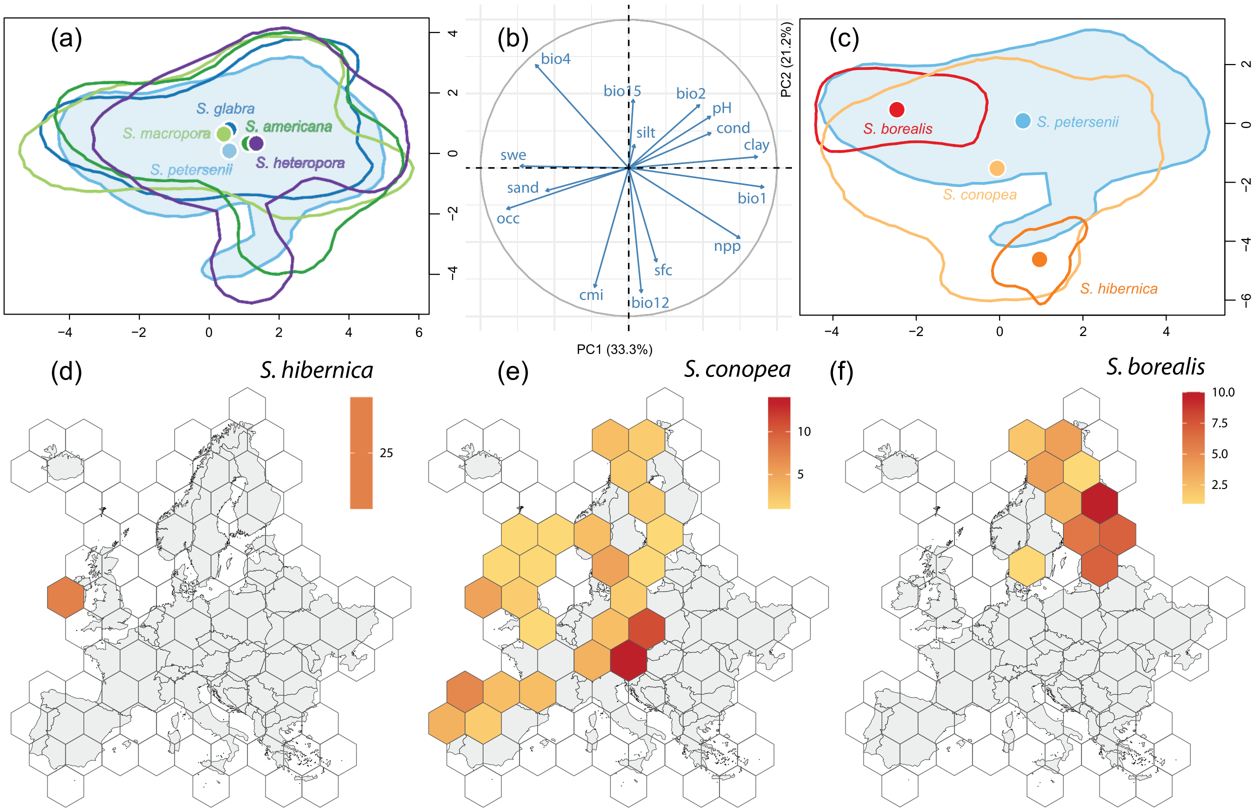

Fig. 3. Climatic niche hypervolumes for the eight most abundant *Synura* species, showing four species with similar (a) and distinct (c) climatic niches compared with *S. petersenii*. PCA (principal component analysis) of uncorrelated 15 Bioclim variables (b), from the left clockwise: cmi, climate moisture index; occ, organic carbon content; sand, sand soil content; swe, snow water equivalent; bio4, temperature seasonality; bio15, precipitation seasonality; silt, silt soil content; bio2, mean diurnal range; pH; cond, conductivity; clay, clay soil content; bio1, annual mean temperature; npp, net primary productivity; sfc, mean monthly near-surface wind speed; bio12, annual precipitation. Distribution of three species with distinct climatic niches across Europe: *S. hibernica* (d), *S. conopea* (e) and *S. borealis* (f).

The highest species diversity was recorded in northern Europe, specifically in Scandinavia and Estonia (Fig. 4a, 4b). Interestingly, the greatest morphological diversity was observed in other parts of Europe, particularly in Greece and the Balkans (Fig. 4c). Consequently, despite the large number of species that occurred in northern Norway and Sweden, they shared a similar morphology of silica scales. The variation in scale length and width does not exhibit a clear biogeographic pattern (Fig. 4d, 4e). However, in the Atlantic region, scales tend to be elongated, while more rounded scales are prevalent in continental Europe (Fig. 4f). Additionally, scales with larger base hole areas are significantly more common in northern Europe (Fig. 4g). Interestingly, the pore size on the keel follows a trend similar to roundness scales, with larger pores being more common in Atlantic Europe (Fig. 4h). Finally, the variability in the distance of struts does not appear to show any specific biogeographic pattern (Fig. 4i).

Effects of environmental variables on morphological traits

A number of environmental variables significantly affected the morphological variability of silica scales (Fig. 5a–f). Of the traits related to scale shape and size, two traits, namely scale length and scale roundness, were found to be significantly dependent on environmental parameters, with R^2 coefficients of 0.12 and 0.16, respectively (Fig. 5b, c). Scale length was negatively correlated with mean diurnal temperature range (bio2) and positively correlated with net primary productivity and soil sand content (Fig. 6a, b). Notably, species with scales longer than 4.5 µm were found only in localities with high sand content. Scale roundness was negatively correlated with annual precipitation (bio12), but positively correlated with annual mean temperature (bio1), temperature seasonality (bio4), climate moisture index (cmi), soil clay content and pH (Fig. 5c). Therefore, species with more circular scales are more likely to occur in areas with lower rainfall and in locations with higher pH (Fig. 6c, 6d).

Traits related to scale pores and holes were also significantly correlated with environmental conditions (Fig. 5d, 5e). The size of the base hole was negatively correlated with temperature variables (bio1, bio2), climate moisture index (cmi) and pH, and positively correlated with the amount of melted snow water, known as the snow water equivalent (swe). It is obvious that species with a large base hole area occur only in cold regions, with

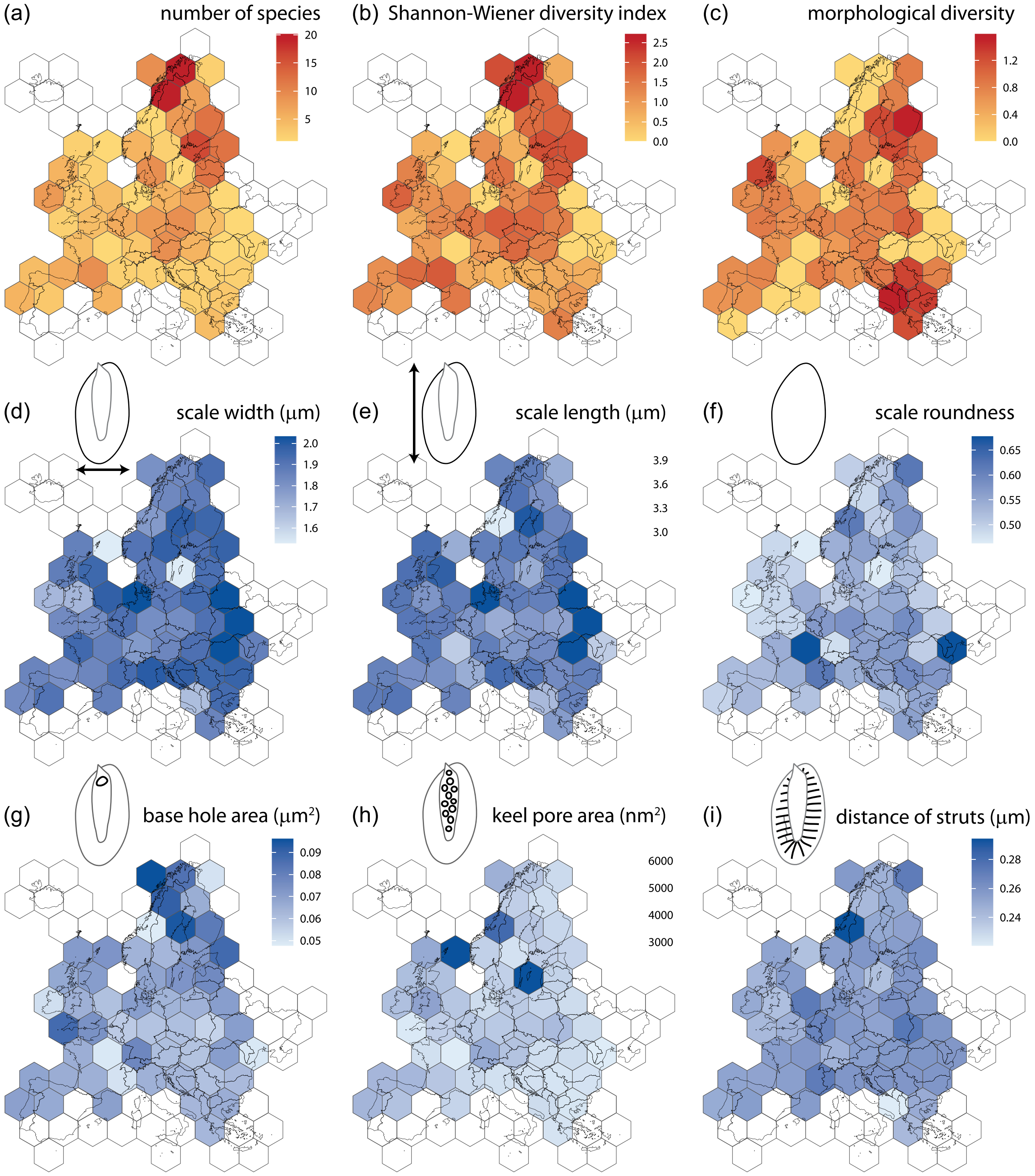

Fig. 4. Distribution patterns of *Synura* species and their morphological traits. Coloured hexagons show areas of Europe where the occurrence of any *Synura* species has been recorded. Three upper maps summarise general diversity patterns, including the number of species (a), Shannon–Wiener diversity index considering species abundance (b) and the diversity of morphological traits of *Synura* silica scales (c). Additional maps (d–i) display the range of selected morphological traits across Europe.

an average annual temperature not exceeding 8°C, and do not occur in areas without snow cover (Fig. 6e, 6f). Keel pore area size was negatively correlated with temperature seasonality (bio4) and positively correlated with annual precipitation (bio12) and the snow water equivalent (swe) (Fig. 5e). Finally, the distance of struts was negatively correlated with annual precipitation (bio12) and positively correlated with annual mean temperature (bio1), climate moisture index (cmi), pH and conductivity (Fig. 5f).

Discussion

This study distinguishes itself by the unprecedented scale of its dataset, encompassing over 700 genetically verified records of a single intrageneric evolutionary

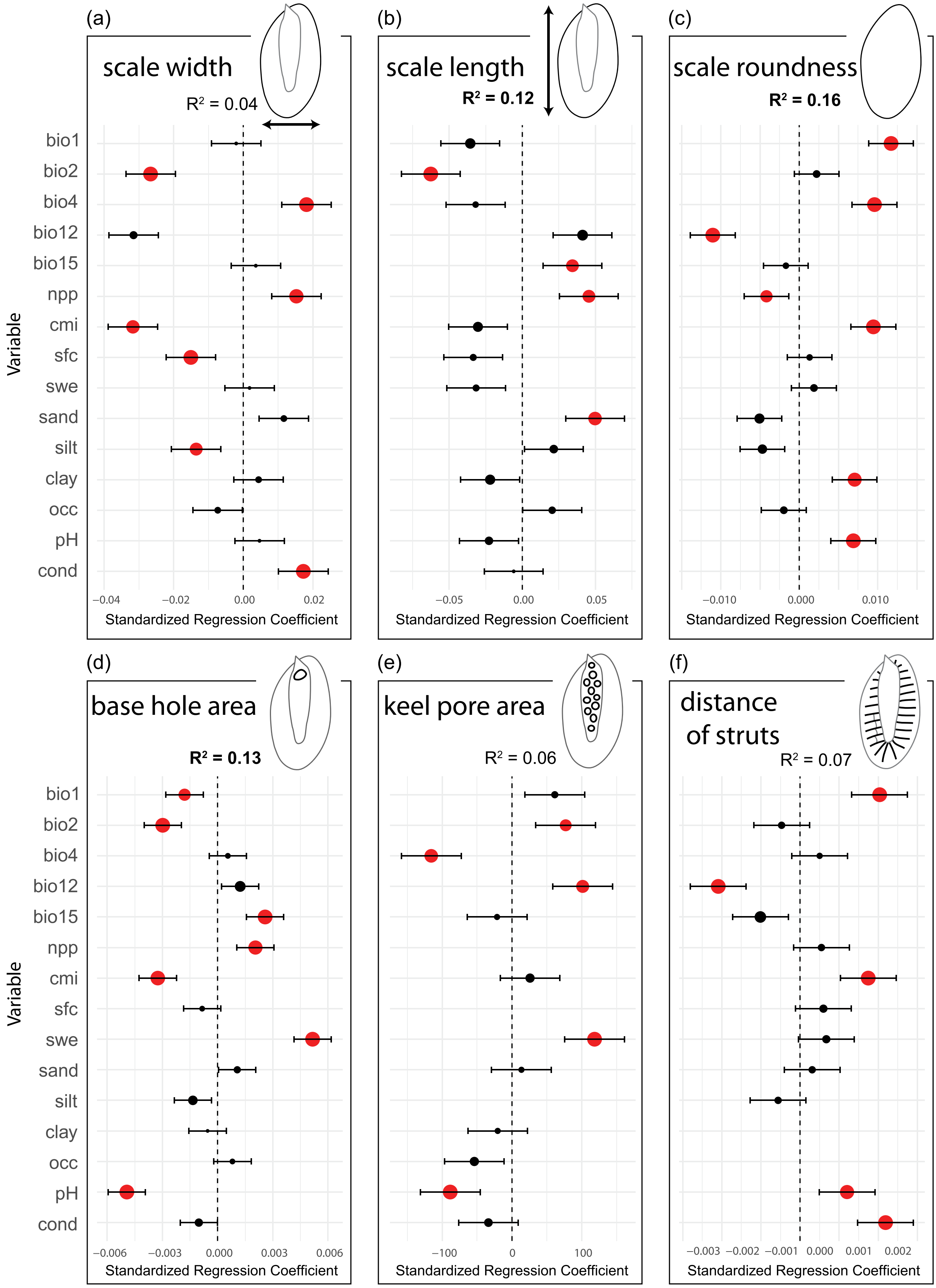

Fig. 5. Effects of environmental variables on morphological traits of *Synura* siliceous scales; scale width (a), scale length (b), scale roundness (c), base hole area (d), keel pore area (e) and distance of struts adjacent to the keel (f). Points represent estimation of standardised regression coefficients, while the error bars correspond to their 95% confidence intervals. Point size is proportional to the relative importance of the given predictor (i.e. the weighted occurrence of the predictor in the set of best models); predictors with importance higher than 0.5 are given in red. The individual predictors are listed as follows: bio1, annual mean temperature; bio2, mean diurnal range; bio4, temperature seasonality; bio12, annual precipitation; bio15, precipitation seasonality; npp, net primary productivity; cmi, climate moisture index; sfc, mean monthly near-surface wind speed; swe, snow water equivalent; sand, sand soil content; silt, silt soil content; clay, clay soil content; occ, organic carbon content; pH; cond, conductivity.

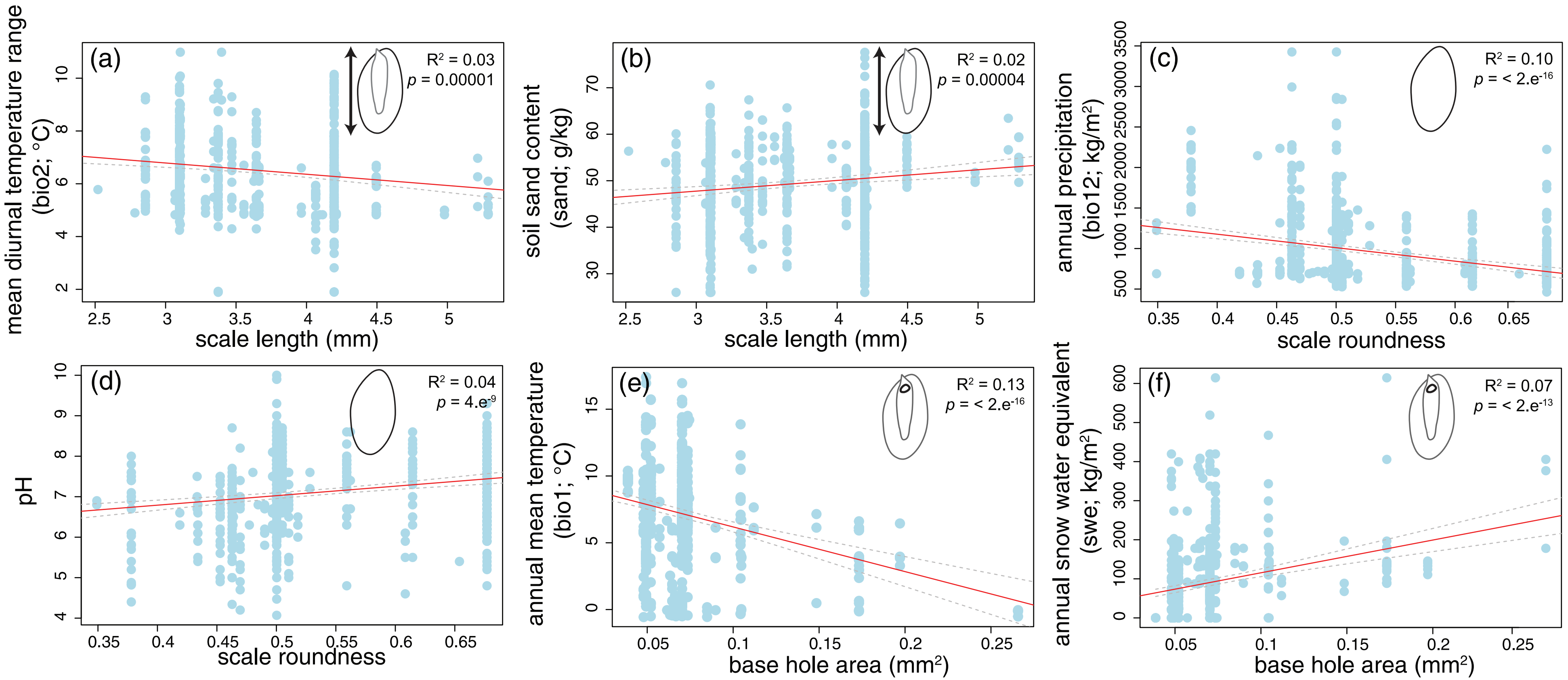

Fig. 6. Linear regression models showing the relationship between the three most informative morphological traits of genus *Synura*; scale length (a, b), scale roundness (c, d) and base hole area (e, f), along with their most powerful predictors.

lineage of eukaryotic microorganisms. By focusing only on closely related species, we have effectively filtered out the influence of the phylogenetic signal, providing an unparalleled depth of understanding regarding the adaptive significance of siliceous scale morphological features. Moreover, this study can be used as a case study for estimating the real diversity of protist genera, pointing out differences in distribution, abundance and rarity of individual species. We acknowledge this work as potentially the most comprehensive pan-European study of its kind on eukaryotic microorganisms to date.

Species diversity, ecology and distribution

The section *Peterseniane* has drawn attention due to its considerable cryptic diversity and wide distribution. The hidden diversity was first brought to our attention by Boo *et al.* (2010) and Kynčlová *et al.* (2010), revealing several lineages with distinct distribution patterns. Subsequent research by Škaloud *et al.* (2012, 2014, 2020) and Jo *et al.* (2016) described new species based on subtle differences in morphology, genetics and ecological traits. Currently comprising 29 species, the section exhibits highly uniform silica scale morphology. Except for four evolutionarily old species (*S. asmundiae*, *S. bjoerkii*, *S. kristiansenii* and *S. macracantha*), most species emerged through adaptive radiation less than 10 million years ago (Siver, 2015; Jadrná *et al.*, 2021). Here, we identified over half of the described *Petersenianae* species (16 out of 29). The remaining species exhibit restricted distribution (e.g. *S. cornuta*, *S. fluviatilis*, *S. kristiansenii*) or are probably very rare. Additionally, we discovered several previously unknown lineages, intriguingly including thermophilic species such as the clade 4, which was exclusively found in Greece.

The most frequently encountered species were *S. petersenii* and *S. glabra* as they occupy a relatively broad ecological niche, thriving in various types of freshwater bodies. These species also demonstrate less sensitivity to pollution and eutrophication compared with other *Synura* species. Interestingly, only three (*S. borealis*, *S. conopea* and *S. hibernica*) of the eight most abundant species can be distinguished by their ecological preferences (Fig. 3a, c). *S. borealis* occurs exclusively in cold regions of northern Europe, with the distribution probably limited by high temperatures during summer (Škaloud *et al.*, 2014). Specifically, it inhabits cold, low-pH waters with temperatures up to 6.5°C. *S. conopea* shows a preference for oligotrophic habitats with low conductivity and is also common in the Atlantic part of Europe, where the mean diurnal temperature range is lower. Finally, *S. hibernica* is exceptional by its very restricted European distribution, occurring exclusively in peat bogs along the western coast of Ireland (Fig. 3d). Among all *Synura* species, *S. hibernica* excels in its strict environmental preferences, preferring low-nutrient, clear water with high carbon content. Proposed as an endemic species, it seems to be uniquely adapted to these specific habitats (Škaloud *et al.*, 2014). Interestingly, the climatic niche of *S. hibernica* was determined by high annual precipitation (Fig. 3b, 3c), and indeed, differences in precipitation intensity have recently been identified as one of the main factors shaping population dynamics and speciation in *Synura* (Škaloud *et al.*, 2024). In brief, precipitation plays a significant role in influencing many other features. It directly impacts abiotic variables, such as pH, conductivity and the amount of dissolved nutrients, and thus indirectly affects the entire phytoplankton community. Additionally, since precipitation undoubtedly affects the amount of nutrients and other sand/clay particles from the environment, it has a great impact on the trophic status, water transparency and light availability. It also has a direct effect on stratification; for example, heavy rain can mix the water column well and rapidly change the proportions of the phytoplankton community. In the case of *S. hibernica*, precipitation may also affect its endemic distribution on the west coast of Ireland, as this region receives specific rainfall with high chloride and sulphate deposition (Beltman *et al.*, 1993).

Despite the chrysophycean species having a wide ecological amplitude and each taxa having a different tolerance of environmental conditions (Roijackers & Kessels, 1986; Siver & Hamer, 1989; Cumming *et al.*, 1992; Siver & Lott, 2017), it is not obvious that any distribution patterns can be recognised. Even an extensive global study did not find any obvious biogeographic patterns or ecological features of genetically defined clades of the genus *Synura* (Boo *et al.*, 2010). However, our data indicate that *Synura* species diversity is increasing northwards, with Scandinavia as the most species-rich region (Fig. 4a, 4b), where the cold temperatures and oligotrophic lakes create highly favourable conditions for a diverse range of *Synura* species (Škaloud *et al.*, 2014). The trend of increasing diversity towards the north in the European context is not very common; for a large number of organisms, the number of species increases southwards with latitudinal gradient (Willig *et al.*, 2003). A large number of water bodies in the area can promote faster diversification of freshwater protists due to the existence of diverse ecological niches leading to resource partitioning and a reduction in competition among newly established species. These niches may include differences in temperature, light availability, nutrient levels and predation pressure. Indeed, Vyverman *et al.* (2007) similarly demonstrated that in northern Europe, local diatom richness positively correlates with lake density. A surprisingly reverse trend is visible for morphological diversity which decreases northwards (Fig. 4c), suggesting that scale morphology in northern Europe is filtered by environmental conditions, forcing organisms to maintain certain morphological parameters (Cornwell *et al*., 2006). A similar proposition has already been stated for the macroorganisms, where functional trait diversity usually has a different distribution from the species diversity (Lamanna *et al*., 2014).

We demonstrated that the occurrence of some morphological traits of silica scales is non-random. For example, there is a clear trend of increasing the base plate hole size towards northern Europe, where rare species with larger base plate holes are more common (Fig. 4g). The trend of bigger struts distance (Fig. 4l) is similar but more subtle due to the large influence of local variables. In addition, *Synura* species with elongated, less rounded scales are more likely to be found in the northwest of Europe (Fig. 4f), where oceanicity is higher. A typical example of such a species with elongated scales and a large base plate hole is *S. hibernica*, which is restricted in its distribution to the western coast of Ireland. Conversely, roundness increases towards southwest Europe, corresponding to increasing continentality. This trend likely reflects the warm climate and predominantly alkaline substrate in southwestern Europe, favouring *Synura* species with rounded scales, a small number of struts, and narrow keels.

Our results are consistent with previous studies on chrysophyte ecology, highlighting the pivotal role of ecological and climatic factors in shaping their distribution (Fig. 3b). Across various studies, pH, temperature, water clarity, colour, conductivity and trophic content (including dissolved nitrogen, phosphorus and carbon) have consistently influenced the occurrence of chrysophyte species (e.g. Roijackers & Kessels, 1986; Dixit & Dixit, 1989; Siver & Hamer, 1989; Cumming *et al*., 1992; Arseneau *et al*., 2016; Siver & Lott, 2017; Tammelin *et al*., 2017; Bock *et al*., 2020). According to our results, *Synura* species occupy seemingly identical ecological niches (Fig. 3a). However, closer examination of the morphological features of their siliceous scales could provide deeper insights into the ecology and distribution of these species while also offering valuable information on trends affecting multiple species concurrently.

Silica scale features as morphological traits in the light of environmental processes

The most important traits for organisms are those impacting their fitness, directly tied to resource acquisition, reproduction and potential protection (Violle *et al*., 2007). Several studies suggest that specific features of silica cover have a significant impact on the overall fitness of algae. For instance, silica frustules of diatoms, when evenly silicified and regularly perforated, may increase light diffraction into the cell interior and directly affect photosynthetic efficiency (Goessling *et al*., 2021). Conversely, a thick silica covering may contribute to reducing dangerous UV-B and UV-A radiation, which could be harmful to the cell (Aguirre *et al*., 2018). A high degree of frustule silicification, as well as the ability to develop silica projections or spines, may potentially reduce grazing (Assmy *et al*., 2013). On the other hand, robust silicification of cell covering contributes to a higher cell mass, resulting in faster sedimentation towards the bottom (Tréguer *et al*., 2018). In addition, spines or projections may decrease diatom buoyancy, and the length of these projections correlates with variations in water osmotic pressure, closely tied to salinity levels (Paasche *et al*., 1975).

For certain morphological traits, their mechanical function remains unclear, but we may observe their association with specific environmental factors. For example, we can examine the ratio of diatom cell symmetry independently of the colony, considering unpredictable conditions of the freshwater stream or prevailing water temperature (Allen, 2014), or discover a strong statistical relationship between diatom valve length and metal contamination (Cattaneo *et al*., 2004).

The morphological traits of *Synura* silica scales are influenced by the underlying architectural principles and structural constraints of the scales, resulting in variability within specific limits (Jadrná *et al*., 2021; Knotek & Škaloud, 2023). When studying the genus *Synura*, we propose focusing on easily measurable traits that align with the traditional criteria used for species delimitation, i.e. overall body scale shape (rounded vs. lanceolate), scale size, keel width and shape, number and spacing of struts, size of base plate and keel pores, and the size of the base plate hole. All of these putative morphological traits are ultrastructural, and we conclude that they may be influenced by environmental conditions.

Scale size

One of the key traits of protists is their size. *In silica* scaled chrysophytes, it has been documented that the size of scales is significantly correlated with the size of the cell (Siver, 2022). Based on our measurements, we have also shown that the same correlation holds for length-width ratios (Supplementary fig. S3). The scale size, which is correlated with the cell size, was identified as a significant factor influenced by ecological variables. Environmental parameters explained 12% of the variation in scale length. Smaller scales were found in regions with a high mean diurnal air temperature range (bio2, Fig. 6a) and low temperature seasonality (bio15, Fig. 5a, 5b). Generally, smaller cells with reduced scales tend to occur at higher temperatures, aligning with the temperature-size rule for protists (Atkinson *et al.*, 2003). One of the reasons for this phenomenon is that cells at higher temperatures have a faster metabolism and divide more rapidly (Savage *et al.*, 2004).

Atlantic Europe exhibits reduced temperature seasonality, but the geographical trend for *Synura* scale sizes is not obvious, probably due to the influence of other predictors (Fig. 4d, 4e). Short-term temperature fluctuations can induce stress, favouring small *Synura* species that can divide rapidly. However, we did not specifically examine the impact of water surface size, which can buffer surrounding temperatures and thus may have a large effect on scale size distribution. In addition, we revealed the effect of nutrient level on the size distribution of *Synura* scales. Longer scales were observed in sites with high dissolved silica (sand used as a proxy) (Fig. 6b), while wider scales were more common in areas with high conductivity (Fig. 5a). Surprisingly, large scales were found in sites with high net primary productivity (NPP, Fig. 5a, 5b). This may suggest that nutrient-rich environments may support the presence of species with larger cells, while small organisms dominate in waters with low nutrient concentrations (Irwin *et al.*, 2006). Specifically, downsizing of chrysophycean genomes and cell sizes can occur in environments with limited nitrogen and phosphate (Olefeld *et al.*, 2018).

Scale shape

We discovered that the roundness of *Synura* scales is significantly affected by ecological variables, with these factors explaining 16% of the variability. Previous studies have already described the relationship between nutrient acquisition, light utilisation, and buoyancy in the water column, directly linked to cell size and shape (Litchman & Klausmeier, 2008; Acevedo-Trejos *et al.*, 2013). When cells are elongated, they exhibit a reduced volume-to-surface ratio, maximising the efficiency of light harvesting and nutrient uptake (Karp-Boss & Boss, 2016). Here, we demonstrated that elongated scales covering surfaces of elongated cells are favoured in regions with low seasonality (bio4; Fig. 5c), typically found in Atlantic Europe (Fig. 4f). Other important factors influencing the scale roundness are annual precipitation, mean air temperature, soil clay content and water pH (Fig. 5c). Elongated cells more efficiently capture available light in regions with frequent rainfall and cloud cover.

We suspect that most of the significant factors together reflect poor nutrient availability. In areas characterised by coarse-grained till, bedrock outcrops and peat deposits, low levels of fine particles like clay or silt indicate natural oligotrophy and low phosphorus content (Tammelin *et al.*, 2017). The combination of clay content and nutrients is removed from the soil through precipitation, as well as from lakes. Elongated cells may offer an evolutionary advantage, as they can more effectively absorb nutrients from the water. This aligns with the fact that we found *Synura* with rounded scales and cells in more eutrophic waters with higher pH (Fig. 6c). These areas typically include flooded regions, dead-end streams or oxbow lakes where rivers introduce nutrients along with subtle clay particles. Geographically, the areas with higher nutrient content are in southern Europe (Fig. 4f), where precipitation is lower and temperature higher, along with seasonality, and so the water bodies are sufficiently nutrient-rich and illuminated. The round cell shape naturally provides better self-shading than elongated cells as the simplest defence against excessive solar radiation (Garcia-Pichel, 1994). A typical example of a species with rounded scales and cells well adapted to higher nutrient levels is *S. glabra*. It can withstand relatively high pH (~8) and conductivity levels (750 μS cm^{-1}). Interestingly, it has been proposed that chrysophytes are not able to thrive in high pH environments as they are not capable of using bicarbonate, which serves as a primary source of carbon in alkaline conditions (Sandgren *et al.*, 1988). Consequently, there is accelerated dissolution of silica at elevated temperature and alkaline pH values, such as in eutrophic habitats (Cappelle & Behrends, 2008; Kuefner *et al.*, 2020; Spitzmüller *et al.*, 2023). However, *S. glabra* clearly manages to somewhat overcome these limitations, possessing the least silicified scales among all other *Synura* species.

In general, cell and scale elongation seems to represent a clear adaptation mechanism for living in oligotrophic waters and areas with reduced sunlight availability. Accordingly, *Synura* species with elongated scales might be at risk due to water eutrophication triggered by agriculture and animal farming.

Base plate hole and keel pores

The area of the base plate hole is a valuable morphological trait, with 13% of its variability explained by environmental factors (Fig. 5d), including low mean annual temperature (Fig. 6e), diurnal temperature range and climate moisture index. Interestingly, the size of keel pores shows a moderate positive correlation with temperature, in contrast to the base plate hole (Fig. 5d, 5e). Both traits are linked to the availability of clean water from melting snow, a geographically related variable (Fig. 4g, 4h, 6f), as well as low pH, resulting in similar distributions (Fig. 4g, h). It is possible that *Synura* in northern and cloudy regions do not require shielding from harmful UV light, allowing them to afford larger holes and pores in their covering. Previous studies have documented that the size of pores on silica coverings can influence the flow of light photons and promote nutrient uptake (Herringer *et al*., 2019; Goessling *et al*., 2021; De Tommasi & Rogato, 2023). However, it is important to note that the base plate hole is positively correlated with the keel width (Jadrná *et al*., 2021) as it is directly associated with keel formation (Wee & Andersen, 1997). Consequently, it is possible that the low pH and the arcto-alpine climate favour the development of large keels in *Synura* scales.

Mean distance between the struts

According to recent research, struts on the *Synura* scales are essential for scale stability, fixing the median keel to the basal plate (Knotek & Škaloud, 2023). The number of struts is therefore strongly correlated with the size of the scale and the keel they support (Jadrná *et al*., 2021). Interestingly, while we also observed the significant relationship between these variables, the mean struts distance represents an independent variable (Supplementary fig. S2), showing a significant relation to some local abiotic factors. Larger distances between struts were observed in water bodies with high conductivity, pH and mean annual air temperature, as well as low annual precipitation amounts (Fig. 5f). These conditions are associated with fast growth and worse silicification of scales (Taylor, 1985; Pančić *et al*., 2019). It is therefore likely that the increasing distance between the struts is an adaptation to low concentrations of silica, which need to be treated sparingly. This leads to less stability of keel fixation, which the organisms seem to cope with by overall reduced silicification of the scales. The distance between struts, as well as the overall degree of silification, may also affect light transmission through the scales or cause light reflection, making it an interesting topic for further research.

Overall, this study establishes a connection between the nanostructures of *Synura* silica scales and species distribution patterns, shedding light on the putative drivers behind them. It serves as a valuable case study for evaluating the true diversity of protist genera and highlights differences in species distribution and abundance. Importantly, we emphasise that even the nanostructures of silica scales can serve as a tool for assessing the fitness of the organism and, consequently, provide insights into the entire freshwater ecosystem. Moreover, trait-based studies like this one have the potential to set up predictions about species distribution patterns, project potential adaptations in response to habitat changes, and provide a glimpse into ongoing morphological evolution.

Acknowledgements

We would like to deeply thank all the collaborators who have participated in the sampling over the years, enabling us to compile the comprehensive database of *Synura* samples, namely Helena Bestová, Dora Čertnerová, Pavla Doskočilová, Evgeniy Gusev, Lucie Jelínková, Petr Knotek, Lucie Křivská, Yvonne Němcová, Anna Procházková, Martin Pusztai, Magda Škaloudová, Zuzana Škvorová, Kateřina Tučková and Václav Uhlík. The authors are very grateful to Peter A. Siver for stimulating discussions.

Disclosure statement

No potential conflict of interest was reported by the author(s).

Funding

This study was supported by the Czech Science Foundation, project No. 20-22346S. Computational resources were provided by the e-INFRA CZ project (ID:90254), supported by the Ministry of Education, Youth and Sports of the Czech Republic.

Supplementary material

The following supplementary material is accessible via the Supplementary Content tab on the article's online page at https://doi.org/10.1080/09670262.2024.2442041.

Supplementary table S1 Origin, sampling details and GenBank accession numbers of analysed strains. The non-European strains used for phylogenetic and morphological analyses only are given in italics.

Supplementary table S2 List of used primers for PCR amplification of three genes ITS rDNA, *cox*1 and *rbcL*.

Supplementary table S3 Complete list with average values of evaluated scale traits of 43 selected *Synura* strains.

Supplementary fig. S1 Correlation plots of the measured morphological traits. Highly correlated traits are delimited by a thick line.

Supplementary fig. S2 Correlation plots of the environmental variables. Highly correlated traits are delimited by a thick line. Variable codes in alphabetical order: bio1 = annual mean temperature, bio2 = mean diurnal range, bio3 = isothermality, bio4 = temperature seasonality, bio5 = max temperature of warmest month, bio6 = min temperature of coldest month, bio7 = temperature annual range, bio8 = mean temperature of wettest quarter, bio9 = mean temperature of driest quarter, bio10 = mean temperature of warmest quarter, bio11 = mean temperature of coldest quarter, bio12 = annual precipitation, bio13 = precipitation of wettest month, bio14 = precipitation of driest month, bio15 = precipitation seasonality, bio16 = precipitation of wettest quarter, bio17 = precipitation of driest quarter, bio18 = precipitation of warmest quarter, bio19 = precipitation of coldest quarter, cat = cation exchange capacity, clay = soil clay content, cmi = mean monthly climate moisture index, gdd0 = growing degree days heat sum above 0°C, gdd5 = growing degree days heat sum above 5°C, gdd10 = growing degree days heat sum above 10°C, gsl = growing season length, npp = net primary productivity, occ = soil organic carbon concentration, ocs = soil organic carbon stock, pet = potential evapotranspiration, rsds = mean monthly surface downwelling shortwave flux in air, sand = soil sand content, sfc = near-surface wind speed, silt = soil silt content, swe = snow water equivalent, vpd = mean monthly vapor pressure deficit.

Supplementary fig. S3 Linear regression model showing the correlation between the length-width ratio of cells and scales.

Data availability statement

Newly obtained sequences were deposited in GenBank (accessions PQ039768–PQ039820, PQ049178–PQ049250). Measured morphological traits are available in the supplementary material. Multiple sequence alignments are available in MendeleyData (https://doi.org/10.17632/79hwpt2c85.1).

Author contributions

I. Jadrná: original concept, drafting and editing manuscript, data curation, formal analysis, investigation; P. Škaloud: review and editing manuscript, data curation, formal analysis, investigation, funding acquisition, resources.

ORCID

Iva Jadrná http://orcid.org/0000-0002-2974-536X
Pavel Škaloud http://orcid.org/0000-0003-1201-3290

References

Acevedo-Trejos, E., Brandt, G., Merico, A. & Smith, S.L. (2013). Biogeographical patterns of phytoplankton community size structure in the oceans. *Global Ecology and Biogeography*, **22**(**9**): 1060–1070.

Ackerly, D.D. & Cornwell, W.K. (2007). A trait–based approach to community assembly: partitioning of species trait values into within-and among-community components. *Ecology Letters*, **10**(**2**): 135–145.

Aguirre, L.E., Ouyang, L., Elfwing, A., Hedblom, M., Wulff, A. & Inganäs, O. (2018). Diatom frustules protect DNA from ultraviolet light. *Scientific Reports*, **8**(**1**): 5138.

Allen, C.S. (2014). Proxy development: a new facet of morphological diversity in the marine diatom *Eucampia antarctica* (*Castracane*) Mangin. *Journal of Micropalaeontology*, **33**(**2**): 131–142.

Arseneau, K.M., Driscoll, C.T., Cummings, C.M., Pope, G. & Cumming, B.F. (2016). Adirondack (NY, USA) reference lakes show a pronounced shift in chrysophyte species composition since ca. 1900. *Journal of Paleolimnology*, **56**: 349–364.

Assmy, P., Smetacek, V., Montresor, M., Klaas, C., Henjes, J., Strass, V.H., Arrieta, J.M., Bathmann, U., Berg, G.M., Breitbarth, E. & Cisewski, B. (2013). Thick-shelled, grazer-protected diatoms decouple ocean carbon & silicon cycles in the iron-limited Antarctic Circumpolar Current. *Proceedings of the National Academy of Sciences*, **110**(**51**): 20633–20638.

Atkinson, D., Ciotti, B.J. & Montagnes, D.J. (2003). Protists decrease in size linearly with temperature: ca. 2.5% C− 1. *Proceedings of the Royal Society of London Series B Biological Sciences*, **270**(**1533**): 2605–2611.

Bartoń, K. (2020). MuMIn: multi-model inference. R package version 1.43.17. https://cran.r-project.org/web/packages/MuMIn/index.html; searched on 20 August 2020.

Beltman, B., Rouwenhorst, G., Whilde, A. & Ten Cate, M. (1993). Chemical composition of rain in Western Ireland. *The Irish Naturalists' Journal*, **24** (**7**): 267–274.

Blonder, B., Lamanna, C., Violle, C. & Enquist, B.J. (2014). The n-dimensional hypervolume. *Global Ecology and Biogeography*, **23**(**5**): 595–609.

Bock, C., Jensen, M., Forster, D., Marks, S., Nuy, J., Psenner, R., Beisser, D. & Boenigk, J. (2020). Factors shaping community patterns of protists & bacteria on a European scale. *Environmental Microbiology*, **22**(**6**): 2243–2260.

Boenigk, J., Pfandl, K. & Hansen, P.J. (2006). Exploring strategies for nanoflagellates living in a 'wet desert'. *Aquatic Microbial Ecology*, **44**(**1**): 71–83.

Boo, S.M., Kim, H.S., Shin, W., Boo, G.H., Cho, S.M., Jo, B. Y., KIM, J.H., Kim, J.H., Yang, E.C., Siver, P.A. & Wolfe, A.P. (2010). Complex phylogeographic patterns in the freshwater alga *Synura* provide new insights into ubiquity vs. endemism in microbial eukaryotes. *Molecular Ecology*, **19**(**19**): 4328–4338.

Bouckaert, R., Vaughan, T.G., Barido-Sottani, J., Duchêne, S., Fourment, M., Gavryushkina, A., KIM, J. H., Kim, J.H., Yang, E.C., Siver, P.A. & Wolfe, A.P. (2019). BEAST 2.5: an advanced software platform for Bayesian evolutionary analysis. *PLOS Computational Biology*, **15**(**4**): e1006650.

Cambon, J., Hernangómez, D., Belanger, C. & Possenriede, D. (2021). tidygeocoder: an R package for geocoding. R package version 1.0.5. https://CRAN.R-project.org/package=tidygeocoder; searched on 20 August 2020.

Cappelle, P.V. & Behrends, T. (2008). Dissolution of biogenic silica from land to ocean: role of salinity and pH. *Limnology and Oceanography*, **53**(**4**): 1614–1621.

Cattaneo, A., Couillard, Y., Wunsam, S. & Courcelles, M. (2004). Diatom taxonomic & morphological changes as indicators of metal pollution & recovery in Lac Dufault (Québec, Canada). *Journal of Paleolimnology*, **32**: 163–175.

Cornwell, W.K., Schwilk, D.W. & Ackerly, D.D. (2006). A trait-based test for habitat filtering: convex hull volume. *Ecology*, **87**(**6**): 1465–1471.

Cumming, B.F., Smol, J.P. & Birks, H.J.B. (1992). Scaled chrysophytes (Chrysophyceae & Synurophyceae) from Adirondack drainage lakes & their relationship to environmental variables. *Journal of Phycology*, **28**(**2**): 162–178.

Darriba, D., Taboada, G.L., Doallo, R. & Posada, D. (2012). jModelTest 2: more models, new heuristics & parallel computing. *Nature Methods*, **9**(**8**): 772.

De Tommasi, E. & Rogato, A. (2023). The Diatom Frustule: morphogenesis and Role in Light Manipulation. *Growth and Form*, **4**((**1–2**)): 3–10.

Dixit, A.S. & Dixit, S.S. (1989). Surface-sediment chrysophytes from 35 Quebec lakes & their usefulness in reconstructing lake-water pH. *Canadian Journal of Botany*, **67**(**7**): 2071–2076.

Ezard, T., Fujisawa, T. & Barraclough, T.G. (2009). Splits: species' limits by threshold statistics. R package version, r29. https://r-forge.r-project.org/projects/splits/; searched on 01 July 2024.

Fernández, L.D., Hernández, C.E., Schiaffino, M.R., Izaguirre, I. & Lara, E. (2017). Geographical distance & local environmental conditions drive the genetic population structure of a freshwater microalga (*Bathycoccaceae*; Chlorophyta) in Patagonian lakes. *FEMS Microbiology Ecology*, **93**(**10**): fix125.

Follows, M.J., Dutkiewicz, S., Grant, S. & Chisholm, S.W. (2007). Emergent biogeography of microbial communities in a model ocean. *Science*, **315**(**5820**): 1843–1846.

Garcia-Pichel, F. (1994). A model for internal self-shading in planktonic organisms & its implications for the usefulness of ultraviolet sunscreens. *Limnology and Oceanography*, **39**(**7**): 1704–1717.

Goessling, J.W., Yanyan, S., Kühl, M. & Ellegaard, M. Frustule photonics & light harvesting strategies in diatoms (2021). In *Diatom Morphogenesis* (V. Annenkov, J. Seckback,& R. Gordon, eds.), 269–300. Wiley, Hoboken, New Jersey, USA.

Green, J.L., Bohannan, B.J. & Whitaker, R.J. (2008). Microbial biogeography: from taxonomy to traits. *Science*, **320**(**5879**): 1039–1043.

Hernangómez, D. & Arel-Bundock, V. (1995). R package 'giscoR': download Map Data from GISCO API – eurostat. R package version 1.43.17. https://cran.r-project.org/web/packages/giscoR/index.html; searched on 20 August 2020.

Herringer, J.W., Lester, D., Dorrington, G.E. & Rosengarten, G. (2019). Can diatom girdle band pores act as a hydrodynamic viral defense mechanism? *Journal of Biological Physics*, **45**: 213–234.

Hurtado, P., Prieto, M., Martínez-Vilalta, J., Giordani, P., Aragón, G., López-Angulo, J., Košuthová, A., Merinero, S., Díaz-Peña, E.M., Rosas, T. & Benesperi, R. (2020). Disentangling functional trait variation & covariation in epiphytic lichens along a continent-wide latitudinal gradient. *Proceedings of the Royal Society B*, **287**(**1922**): 20192862.

Irwin, A.J., Finkel, Z.V., Schofield, O.M. & Falkowski, P.G. (2006). Scaling-up from nutrient physiology to the size-structure of phytoplankton communities. *Journal of Plankton Research*, **28**(**5**): 459–471.

Jadrná, I., Siver, P.A. & Škaloud, P. (2021). Morphological evolution of silica scales in the freshwater genus *Synura* (Stramenopiles). *Journal of Phycology*, **57**(**1**): 355–369.

Jo, B.Y., Kim, J.I., Škaloud, P., Siver, P.A. & Shin, W. (2016). Multigene phylogeny of *Synura* (Synurophyceae) & descriptions of four new species based on morphological & DNA evidence. *European Journal of Phycology*, **51**(**4**): 413–430.

Jones, G. (2016). Tests on priors for STACEY 1.1.

Jones, G., Aydin, Z. & Oxelman, B. (2015). DISSECT: an assignment-free Bayesian discovery method for species delimitation under the multispecies coalescent. *Bioinformatics*, **31**(**7**): 991–998.

Karger, D.N. & Zimmermann, N.E. (2021). Climatologies at high resolution for the earth land surface areas CHELSA V1. 2: technical specification.

Karp-Boss, L. & Boss, E. (2016). The elongated, the squat & the spherical: selective pressures for phytoplankton shape. In *Aquatic Microbial Ecology & Biogeochemistry: A Dual Perspective* (Glibert P. M. & Kana T. M., eds.), 25–34. Heidelberg, Germany: Springer.

Katoh, K., Misawa, K., Kuma, K.I. & Miyata, T. (2002). MAFFT: a novel method for rapid multiple sequence alignment based on fast Fourier transform. *Nucleic Acids Research*, **30**(**14**): 3059–3066.

Knotek, P. & Škaloud, P. (2023). The effect of patterned structures on the mechanical resistance of microscopic silica scales. *Fottea*, **23**(**2**): 190–200.

Kuefner, W., Ossyssek, S., Geist, J. & Raeder, U. (2020). The silicification value: a novel diatom-based indicator to assess climate change in freshwater habitats. *Diatom Research*, **35**(**1**): 1–16.

Kynčlová, A., Škaloud, P. & Škaloudová, M. (2010). Unveiling hidden diversity in the *Synura petersenii* species complex (Synurophyceae, Heterokontophyta). *Nova Hedwigia Beiheft*, **136**: 283–298.

Lamanna, C., Blonder, B., Violle, C., Kraft, N.J., Sandel, B., Šímová, I., Donoghue, J.C., Svenning, J.C., McGill, B.J., Boyle, B. & Buzzard, V. (2014). Functional trait space & the latitudinal diversity gradient. *Proceedings of the National Academy of Sciences*, **111**(**38**): 13745–13750.

Litchman, E. & Klausmeier, C.A. (2008). Trait-based community ecology of phytoplankton. *Annual Review of Ecology, Evolution, and Systematics*, **39**(**1**): 615–639.

Mašková, T., Herben, T., Hošková, K. & Koubek, T. (2022). Shoot senescence in herbaceous perennials of the temperate zone: identifying drivers of senescence pace & shape. *Journal of Ecology*, **110**(**6**): 1296–1311.

Merico, A., Bruggeman, J. & Wirtz, K. (2009). A trait-based approach for downscaling complexity in plankton ecosystem models. *Ecological Modelling*, **220**(**21**): 3001–3010.

Nguyen, L.T., Schmidt, H.A., Von Haeseler, A. & Minh, B. Q. (2015). IQ-TREE: a fast & effective stochastic algorithm for estimating maximum-likelihood phylogenies. *Molecular Biology & Evolution*, **32**(**1**): 268–274.

Olefeld, J.L., Majda, S., Albach, D.C., Marks, S. & Boenigk, J. (2018). Genome size of chrysophytes varies with cell size & nutritional mode. *Organisms Diversity and Evolution*, **18**: 163–173.

Paasche, E., Johansson, S. & Evensen, D.L. (1975). An effect of osmotic pressure on the valve morphology of the diatom *Skeletonema subsalsum* (A.Cleve) Bethge. *Phycologia*, **14**(**4**): 205–211.

Pančić, M. & Kiørboe, T. (2018). Phytoplankton defence mechanisms: traits & trade-offs. *Biological Reviews*, **93** (**2**): 1269–1303.

Pančić, M., Torres, R.R., Almeda, R. & Kiørboe, T. (2019). Silicified cell walls as a defensive trait in diatoms. *Proceedings of the Royal Society B*, **286**(**1901**): 20190184.

Pateiro-Lopez, B. & Rodriguez-Casal, A. (2016). Alphahull: generalization of the Convex Hull of a Sample of Points in the Plane. https://cran.r-project.org/package=alphahull; searched on 01 July 2024.

Pebesma, E. & Bivand, R. (2023). Spatial data science: with applications in R. https://CRAN.R-project.org/package=sf; searched on 20 August 2020.

Pigot, A.L., Sheard, C., Miller, E.T., Bregman, T.P., Freeman, B.G., Roll, U., Seddon, N., Trisos, C.H., Weeks, B.C. & Tobias, J.A. (2020). Macroevolutionary convergence connects morphological form to ecological function in birds. *Nature Ecology and Evolution*, **4**(**2**): 230–239.

Plante, C.J., Hill-Spanik, K., Cook, M. & Graham, C. (2021). Environmental & spatial influences on biogeography & community structure of saltmarsh benthic diatoms. *Estuaries and Coasts*, **44**: 147–161.

Poggio, L., De Sousa, L.M., Batjes, N.H., Heuvelink, G.B., Kempen, B., Ribeiro, E. & Rossiter, D. (2021). SoilGrids 2.0: producing soil information for the globe with quantified spatial uncertainty. *Soil*, **7**(**1**): 217–240.

Puillandre, N., Lambert, A., Brouillet, S. & Achaz, G.J.M.E. (2012). ABGD, Automatic Barcode Gap Discovery for primary species delimitation. *Molecular Ecology*, **21**(**8**): 1864–1877.

Rambaut, A., Drummond, A.J., Xie, D., Baele, G. & Suchard, M.A. (2018). Posterior summarisation in Bayesian phylogenetics using Tracer 1.7. *Systematic Biology*, **67**(**5**): 901–904.

Rasband, W.S. (1997). Imagej, U. S. National Institutes of Health, Bethesda, Maryland, USA https://imagej.nih.gov/ij/; searched on 12 October 2020.

R Core Team (2020). R: a language & environment for statistical computing. Vienna, Austria: R Foundation for Statistical Computing. https://www.R-project.org/; searched on 01 July 2024.

Roijackers, R.M.M. & Kessels, H. (1986). Ecological characteristics of scale-bearing Chrysophyceae from The Netherlands. *Nordic Journal of Botany*, **6**(**3**): 373–385.

Salzburger, W. (2009). The interaction of sexually & naturally selected traits in the adaptive radiations of cichlid fishes. *Molecular Ecology*, **18**(**2**): 169–185.

Sandgren, C.D. (1988) The Ecology of Chrysophyte Flagellates: Their Growth and Perennation Strategies As Freshwater Phytoplankton. In *Growth and Reproductive Strategies of Freshwater Phytoplankton* (Sandgren, C.D., editor), 9–104. Cambridge University Press, Cambridge.

Savage, V.M., Gillooly, J.F., Brown, J.H., West, G.B. & Charnov, E.L. (2004). Effects of body size & temperature on population growth. *The American Naturalist*, **163**(**3**): 429–441.

Siver, P.A. (2022). The downsizing of gigantic scales & large cells in the genus *Mallomonas* (*Synurales*, Chrysophyceae). *Scientific Reports*, **12**(**1**): 4896.

Siver, P.A. & Hamer, J.S. (1989). Multivariate statistical analysis of the factors controlling the distribution of scaled chrysophytes. *Limnology and Oceanography*, **34** (**2**): 368–381.

Siver, P.A., Jo, B.Y., Kim, J.I., Shin, W., Lott, A.M. & Wolfe, A.P. (2015). Assessing the evolutionary history of the class Synurophyceae (Heterokonta) using molecular, morphometric, & paleobiological approaches. *American Journal of Botany*, **102**(**6**): 921–941.

Siver, P.A. & Lott, A.M. (2017). The scaled chrysophyte flora in freshwater ponds & lakes from Newfoundland, Canada, & their relationship to environmental variables. *Cryptogamie, Algologie*, **38**(**4**): 325–347.

Škaloud, P., Jadrná, I., Dvořák, P., Škvorová, Z., Pusztai, M., Čertnerová, D., Bestová, H. & Rengefors, K. (2024). Rapid diversification of a free-living protist is driven by adaptation to climate & habitat. *Current Biology*, **34**(**1**): 92–105.

Škaloud, P., Kristiansen, J. & Škaloudová, M. (2013). Developments in the taxonomy of silica-scaled chrysophytes–from morphological & ultrastructural to molecular approaches. *Nordic Journal of Botany*, **31**(**4**): 385–402.

Škaloud, P., Kynčlová, A., Benada, O., Kofroňová, O. & Škaloudová, M. (2012). Toward a revision of the genus *Synura*, section *Petersenianae* (Synurophyceae, Heterokontophyta): morphological characterization of six pseudo-cryptic species. *Phycologia*, **51**(**3**): 303–329.

Škaloud, P., Škaloudová, M., Jadrná, I., Bestová, H., Pusztai, M., Kapustin, D. & Siver, P.A. (2020). Comparing morphological & molecular estimates of species diversity in the freshwater genus *Synura* (Stramenopiles): a model for understanding diversity of eukaryotic microorganisms. *Journal of Phycology*, **56**(**3**): 574–591.

Škaloud, P., Škaloudová, M., Procházková, A. & Němcová, Y. (2014). Morphological delineation & distribution patterns of four newly described species within the *Synura petersenii* species complex (Chrysophyceae, Stramenopiles). *European Journal of Phycology*, **49**(**2**): 213–229.

Spitzmüller, L., Nitschke, F., Rudolph, B., Berson, J., Schimmel, T. & Kohl, T. (2023). Dissolution control and stability improvement of silica nanoparticles in aqueous media. *Journal of Nanoparticle Research*, **25**(**3**): 40.

Suchard, M.A., Lemey, P., Baele, G., Ayres, D.L., Drummond, A.J. & Rambaut, A. (2018). Bayesian phylogenetic & phylodynamic data integration using BEAST 1.10. *Virus Evolution*, **4**(**1**): vey016.

Tammelin, M., Kauppila, T. & Viitasalo, M. (2017). Factors controlling recent diatom assemblages across a steep local nutrient gradient in central-eastern Finland. *Hydrobiologia*, **799**: 309–325.

Taylor, N.J. (1985). Silica incorporation in the diatom *Coscinodiscus granii* as affected by light intensity. *British Phycological Journal*, **20**(**4**): 365–374.

Tréguer, P., Bowler, C., Moriceau, B., Dutkiewicz, S., Gehlen, M., Aumont, O., Bittner, L., Dugdale, R., Finkel, Z., Iudicone, D. & Jahn, O. (2018). Influence of diatom diversity on the ocean biological carbon pump. *Nature Geoscience*, **11**(**1**): 27–37.

Violle, C., Navas, M.L., Vile, D., Kazakou, E., Fortunel, C., Hummel, I. & Garnier, E. (2007). Let the concept of trait be functional! *Oikos*, **116**(**5**): 882–892.

Vyverman, W., Verleyen, E., Sabbe, K., Vanhoutte, K., Sterken, M., Hodgson, D.A., Mann, D.G., Juggins, S., Van de Vijver, B., Jones, V., Flower, R., Roberts, D., Chepurnov, V.A., Kilroy, C., Vanormelingen, P. & De Wever, A. (2007). Historical processes constrain patterns in global diatom diversity. *Ecology*, **88**(**8**): 1924–1931.

Wee, J.L. & Andersen, R.A. (1997). Scale Biogenesis in Synurophycean Protists: phylogenetic Implications. *Critical Reviews In Plant Sciences*, **16**(**6**): 497–534.

Wei, T. & Simko, V. (2021). R package 'corrplot': visualization of a Correlation Matrix. R package version 0.92. https://cran.r-project.org/web/packages/corrplot/index.html; searched on 11 July 2024.

Westerband, A.C., Funk, J.L. & Barton, K.E. (2021). Intraspecific trait variation in plants: a renewed focus on its role in ecological processes. *Annals of Botany*, **127** (**4**): 397–410.

Wickham, H., Chang, W., Henry, L., Pedersen, T.L., Takahashi, K., Wilke, C., Woo, K. & Yutani, H. (2019). ggplot2: elegant Graphics for Data Analysis. R package version 1.43.17. https://CRAN.R-project.org/package=ggplot2; searched on 20 Aug 2020.

Willig, M.R., Kaufman, D.M. & Stevens, R.D. (2003). Latitudinal gradients of biodiversity: pattern, process, scale, & synthesis. *Annual Review of Ecology, Evolution, and Systematics*, **34**(**1**): 273–309.

Zhang, H., Huang, X., Huang, L., Bao, F., Xiong, S., Wang, K. & Zhang, D. (2018). Microeukaryotic biogeography in the typical subtropical coastal waters with multiple environmental gradients. *Science of the Total Environment*, **635**: 618–628.

Zhang, J., Kapli, P., Pavlidis, P. & Stamatakis, A. (2013). A general species delimitation method with applications to phylogenetic placements. *Bioinformatics*, **29**(**22**): 2869–2876.